Nuclear and Emerging Technologies for Space, American Nuclear Society Topical Meeting
Richland, WA, February 25 – February 28, 2019, available online at http://anstd.ans.org/

INCREASED PLUTONIUM-238 PRODUCTION VIA HIGH FLUX ISOTOPE REACTOR PERMANENT BERYLLIUM REFLECTOR REDESIGN[1]

D. Chandler, M. W. Crowell, and K. E. Royston

Oak Ridge National Laboratory, P.O. Box 2008, Oak Ridge, TN, 37831-6399, USA
chandlerd@ornl.gov

Irradiation of ^{237}Np-bearing targets in the permanent beryllium reflector (PBR) of Oak Ridge National Laboratory's (ORNL) High Flux Isotope Reactor (HFIR) results in high-purity ^{238}Pu that can be used as a reliable power source for deep space and planetary National Aeronautics and Space Administration missions. However, HFIR's ^{238}Pu production capability is constrained by the available irradiation volume in its PBR. In preparation for the HFIR beryllium change-out in 2023, ORNL staff have redesigned the PBR to include six additional irradiation sites, be more versatile with respect to irradiation and scattering experiments, and enhance its thermal-structural performance. The new PBR design offers large potential increases in annual ^{238}Pu production at ORNL.

I. INTRODUCTION

A technology demonstration sub-project was initiated at the Oak Ridge National Laboratory (ORNL) to develop and implement the technology required to establish a new ^{238}Pu supply chain in support of the US Department of Energy (DOE) and National Aeronautics and Space Administration (NASA) reestablishing a domestic ^{238}Pu production program.[1] Three of the primary steps required to produce ^{238}Pu include ^{237}Np pellet-bearing target fabrication at the Radiochemical Engineering Development Center (REDC), target irradiation in the High Flux Isotope Reactor's (HFIR) permanent beryllium reflector (PBR) vertical experiment facilities (VXF), and chemical processing and recovery at REDC.

This paper summarizes recent efforts in redesigning HFIR's PBR to be more versatile with respect to its multi-mission scientific objectives including neutron scattering and ^{238}Pu production and to enhance its thermal-structural performance. Analyses illustrating large potential increases in annual ^{238}Pu production are highlighted.

I.A. Plutonium-238 Production and Usage

Neutron capture in the ^{237}Np nucleus produces ^{238}Np, which beta-decays with a half-life of 2.12 days into ^{238}Pu. ^{238}Pu, in the form of PuO_2, is used as a reliable power source for deep space and planetary NASA missions. Loaded with PuO_2 fuel, a radioisotope thermoelectric generator converts the heat energy produced from the alpha-decay of ^{238}Pu into useable electricity.

I.B. High Flux Isotope Reactor

HFIR is a US DOE Office of Science User Facility that provides one of the highest steady-state neutron fluxes of any research reactor in the world. The primary missions of this versatile beryllium reflected, light-water-cooled and -moderated, flux-trap type reactor include cold and thermal neutron scattering, isotope production, and materials irradiation/testing. The reactor is loaded with ~ 9.4 kg ^{235}U (high-enriched uranium U_3O_8-Al fuel), operates at 85 MW, provides a peak unperturbed thermal flux of ~ 2.5x10^{15} n/cm^2-s, and typically operates for 24 to 26 days per cycle.

The HFIR core (Figure 1) consists of a series of annular regions including a flux trap, two fuel elements composed of involute-shaped fuel plates, two control elements, and a ring of beryllium composed of a removable reflector, a semi-permanent reflector, and a PBR. The PBR contains 22 VXFs used for irradiation experiments, two pneumatic tubes (PT) used for neutron activation analysis, and four horizontal beam (HB) tubes that deliver cold and thermal neutrons to scattering instruments.

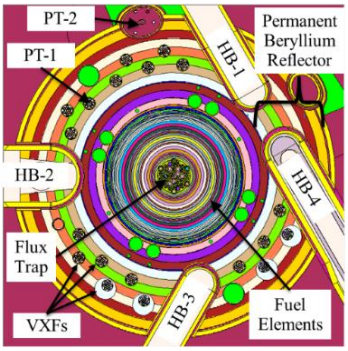

Fig. 1. HFIR MCNP model at core horizontal midplane.

I.B.1. Current Beryllium Reflector Design

PBR no. 4 (Figure 2) has 22 VXFs that are located concentric with the core on three circles of radii. The bolt

circle radii of the 11 inner small VXFs (ISVXF), five outer small VXFs (OSVXF), and six large VXFs (LVXF) are 39.21, 44.05, and 46.28 cm, respectively. The outer radii of the small and large VXFs are 2.22 and 3.81 cm and the inner radii of their aluminum liners are 2.01 and 3.60 cm. The angle of separation between adjacent VXFs on the same bolt circle is 18°. PT-1 is in ISVXF-7 and its piping system runs directly above LVXF-6, rendering it unusable. PT-2 is in engineering facility no. 2 (EF-2).

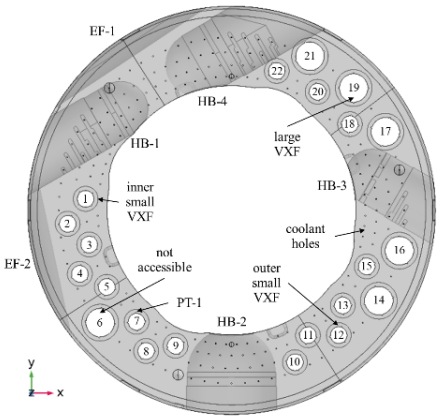

Fig. 2. Permanent reflector no. 4 design.

PBR no. 4 is cooled by water that flows axially downward through 0.16-cm-radius holes and grooves. The 198 cooling holes are located on four bolt circles concentric with the core, each containing holes spaced on 4.5° intervals, except where they would interfere with experiment facilities. The 83 cooling grooves cut into the walls of the 22 VXFs roughly correspond with the array of cooling holes. The ISVXF, OSVXF, and LVXF hole walls have four, three, and four grooves, respectively.

II. PERMANENT REFLECTOR DESIGN STUDIES

The lifetime of a PBR is ~ 279 GWd (~125 – 135 cycles) and PBR no. 4 is scheduled to be replaced with PBR no. 5 in 2023. This replacement therefore represents a rather infrequent opportunity to update and improve on the design. In preparation for this activity, ORNL staff have redesigned the PBR to (1) increase its versatility for experiments, (2) increase the potential ^{238}Pu production capability, (3) arrange the VXFs so as to maintain or increase neutron fluxes down the HB tubes for neutron scattering, (4) enhance its thermal-structural performance, and (5) simplify the fabrication process where possible to reduce machining time, cost, and associated risk.

HFIR is a multi-purpose machine and therefore the new PBR must not negatively affect existing missions. Programmatic requirements have been set to limit cycle length reductions and HB tube flux perturbations caused by experiments to 12 hours and 5%, respectively. Additionally, the temperature and stress distributions of the new PBR must be improved relative to the current design to reduce stress cracking features, which could potentially increase its in-service lifetime. Detailed neutronics and thermal-structural analyses were performed to optimize the PBR design with respect to the defined improvement areas while considering the predefined design constraints.

II.A. Redesign Neutronics Calculations

The neutronics toolset includes the MCNP[2] Monte Carlo-based transport code, the ADVANTG[3] variance reduction tool, the SCALE[4] ORIGEN point depletion and decay code, and the VESTA[5] depletion tool making use of MCNP and ORIGEN 2.2.[6] The MCNP models employed are based on those described in Refs. 1, 7, and 8.

II.A.1. Plutonium-238 Evaluations

PuO_2 production studies were performed to estimate potential increases with respect to the number of VXFs, number of targets per VXF, feed material form (cermet or oxide), bolt circle radii on which the VXFs reside, and number split between OSVXFs and LVXFs. Sensitivity of the target efficiency and product quality to these design variables was also studied. Figure 3 provides two examples of concept layouts with varying degrees of separation.

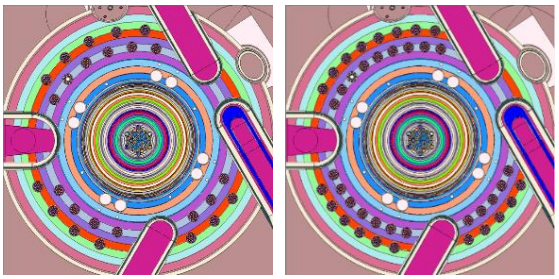

Fig. 3. MCNP models with VXFs azimuthally separated by 15° (left) and 10° (right).

A Python activation script[1,7] coupling the MCNP and SCALE ORIGEN codes was used along with the ADVANTG tool in these studies. The results qualitatively proved that, within the design space explored, the more initial ^{237}Np loaded in the reflector, the more ^{238}Pu is produced. However, target efficiency, in terms of ^{238}Pu per target, reduces considerably with increased ^{237}Np loadings due to self-shielding effects.

II.A.2. Cycle Length Penalty Evaluations

Experiments may not reduce the reactor cycle length by more than 12 hours and therefore the number of considered VXFs should not exceed the number resulting in a penalty of ~ 12 hours when loaded with experiments. Cycle length reduction calculations were performed with VESTA and a criticality search script[9] for several concept designs with various design variables. An example of the control element withdrawal curves, which dictate the cycle length, for the reference case (current reflector, no experiments) and a perturbed case (a concept design, all VXFs loaded with oxide targets) is provided in Figure 4.

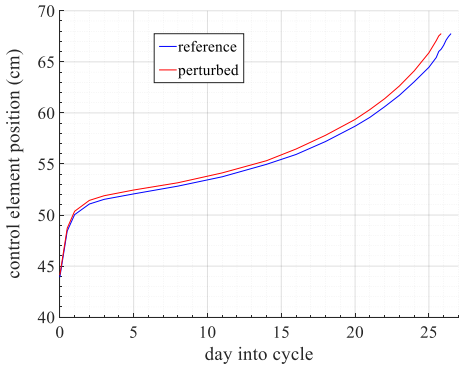

Fig. 4. Control element withdrawal curves.

II.A.3. Beam Tube Flux Evaluations

Experiments may not perturb the fluxes down the HB tubes by more than 5% and therefore the location of the VXFs with respect to the HB tubes must be carefully considered to maximize the availability of the VXFs for ^{238}Pu production targets. The potential impact on the fluxes is twofold: the instruments could see a reduction in low-energy neutrons due to absorption in the targets and an increase in fast neutrons due to fission in the targets.

The ADVANTG and MCNP codes were used to analyze a reference case with no targets and numerous configurations in which the VXF locations and target types (cermet or oxide) were perturbed. Detailed spectra were obtained using point detectors and angularly binned surface tallies at varying distances down each of the four HB tubes. An example of the neutron flux for the reference case and a perturbed case is provided in Figure 5.

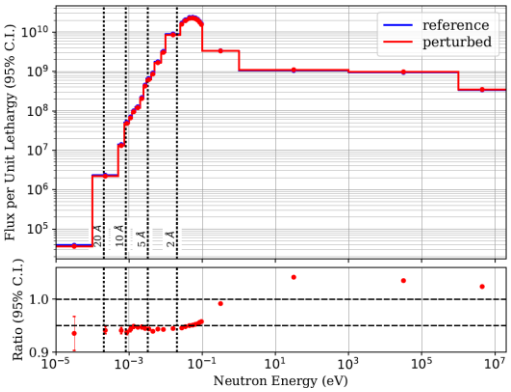

Fig. 5. Neutron flux spectra comparison.

II.A.4. Heat Deposition Evaluations

Heat deposition calculations were performed with MCNP for input to thermal-structural analyses. Various VXF loadings including ^{238}Pu targets, Be plugs, Al plugs, and water/SST liners were analyzed. The heat deposition profiles across the PBR were utilized in determining updated coolant hole bolt circle radii. Heat deposition results are provided for a concept design in Figure 6.

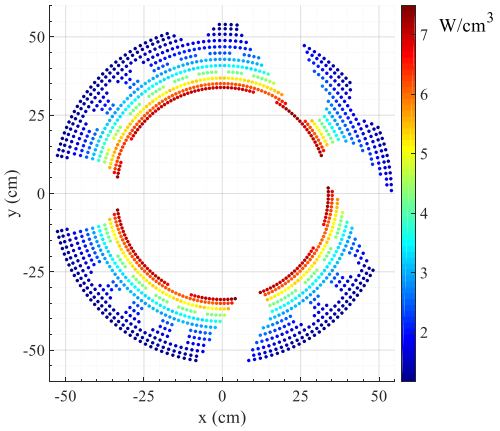

Fig. 6. Heat deposition at core midplane.

II.B. Redesign Thermal-Structural Calculations

The COMSOL Multiphysics[10] finite element analysis software was employed for high-fidelity 3-D thermal-structural evaluations of the PBR. The PBR no. 4 thermal-structural performance is not optimal because of limitations in the original design and the updates to some aspects of the design and not others. For example, VXFs 21 and 22 nearly intersect the HB-4 cutout, which was increased in size in the early 2000s, creating unnecessarily thin webs of reflector material at the reactor midplane.

Analyses of PBR no. 4, using the updated analysis tools and computing platforms currently available, indicated that the heating combined with the coolant distribution induces a significant positive temperature gradient from the reflector ID to OD. This drives generally compressive stresses near the OD and tensile stresses near the ID. Tensile stresses near the reflector ID, where it suffers the highest rate of irradiation damage, are particularly undesirable as they are likely to limit the reflector lifetime. Temperature distributions for the PBR no. 4 and no. 5 designs are provided in Figure 7.

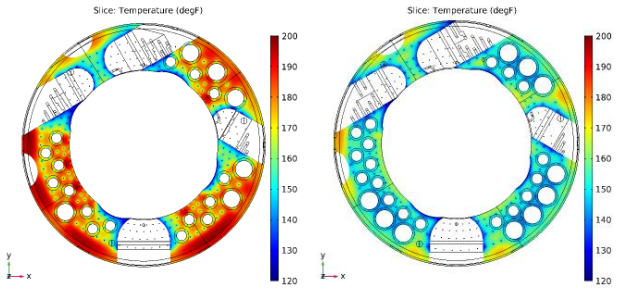

Fig. 7. Midplane temperature (°F) distributions for the permanent reflector no. 4 (left) and no. 5 (right) designs.

II.C. Permanent Beryllium Reflector No. 5 Design

The neutronics results indicated that an azimuthal angle of no less than ~ 13° separation should be regarded when simultaneously considering production efficiency,

cycle length penalties, and HB tube fluxes. The flux studies provided guidelines on locations where VXFs may be placed without adversely affecting the fluxes. Relocating PT-1 to an ISVXF adjacent to HB-2 was also suggested to minimize perturbations to PT-1 and HB-2 due to surrounding targets. Additionally, the production studies showed that OSVXFs result in greater ^{238}Pu production than LVXFs. A near finalized layout was then created.

The thermal-structural studies, which sought to enhance the temperature and stress profiles by optimizing the coolant distribution and eliminating stress riser features, ultimately led to the final design of PBR no. 5 (Figure 8). The VXF spacing was set at 13.1° with the inner and outer rows offset by 6.55° to balance structural integrity with optimized neutronics. Based on the thermal-structural results and feedback from the HFIR Experiment Group, it was decided to maximize the number of LVXFs to increase the reflector's flexibility for all experiment types. This yielded a total of 15 ISVXFs, three OSVXFs, and 10 LVXFs. The bolt circle radius of the ISVXFs was maintained while the bolt circle radius of the LVXFs was increased slightly and that of the OSVXFs was increased more significantly to maintain structural integrity and align the inner edges of the OSVXFs and LVXFs.

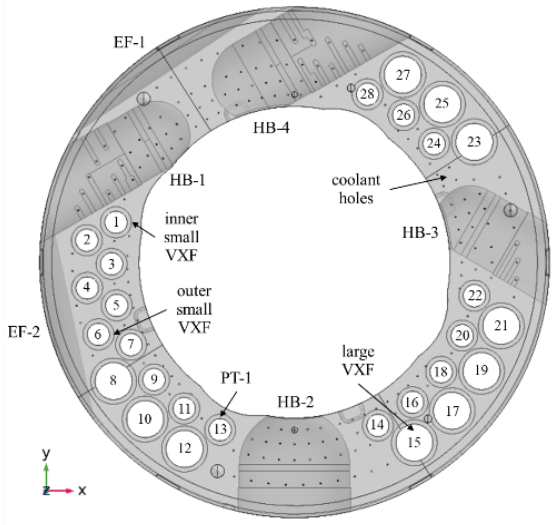

Fig. 8. Permanent reflector no. 5 design.

While the IDs of the VXF liners were maintained, the VXF holes in the reflector were slightly enlarged to enable moving the coolant slots from the reflector to the liners. The number of coolant slots per VXF was also increased from 3 – 4 to 12 to align with the existing 12 coolant inlets in the VXF liner tophats. The bolt circle radius of the outermost circle of 0.16-cm-radius coolant holes was increased to correspond more closely with equal heat deposition bands in the reflector. Also, a 2.25° spacing layout was used with holes typically placed at every 2nd grid point (4.5° spacing) or, where necessary, at every 3rd grid point (6.75° spacing). This more flexible layout helped to avoid the issues with the intersections with HB tube cutouts found throughout the current no. 4 design without creating large uncooled areas of the reflector.

III. DESIGN IMPACT ON PuO_2 PRODUCTION

To demonstrate the impact of the new reflector design on PuO_2 production, four configurations were modeled: PBR no. 4 maximum (Figure 1), PBR no. 4 constrained, PBR no. 5 maximum, and PBR no. 5 constrained (Figure 9). All cases modeled seven fully loaded targets, each containing cermet pellets (20 vol.% NpO_2, 70% Al, 10% void), per VXF. The maximum configurations utilize all the accessible VXFs less those that result in HB tube flux penalties greater than 5%. For the constrained configurations, it is assumed that negligible impact to HB and PT fluxes can take place and two ISVXFs, one OSVXF, and two LVXFs must be available for other experiments. Table I lists the number of VXFs modeled with ^{238}Pu production targets for each configuration.

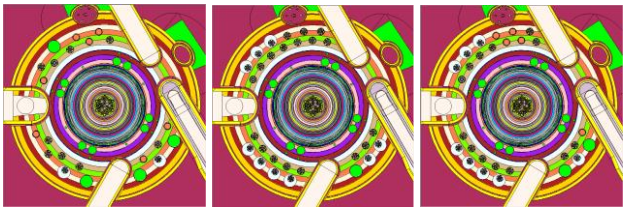

Fig. 9. Permanent reflector no. 4 constrained (left), no. 5 maximum (middle), and no. 5 constrained (right).

TABLE I. Number of VXFs loaded with ^{238}Pu targets.

PBR	Configuration	ISVXF	OSVXF	LVXF
no. 4	maximum	10	4	4
no. 4	constrained	6	2	2
no. 5	maximum	14	3	9
no. 5	constrained	11	1	8

Because of the more optimized PBR no. 5 VXF layout with respect to HB tube fluxes, some VXFs adjacent to HB tubes are assumed to have negligible impacts to HB tube fluxes if loaded with non-absorbing experiments. The reactor cycle length is assumed to be 25 days for all cases analyzed although there will be small differences (i.e., few hours) between the four configurations analyzed. More detailed simulations confirming the assumptions made in these studies and incorporating cycle lengths specific to each configuration will be performed later. Furthermore, the configurations modeled and discussed will need to be vetted through safety-related calculations.

Table II lists the reflector design and configuration dependent results assuming the targets in the ISVXFs, OSVXFs, and LVXFs remain in the reactor for three, six, and six consecutive cycles, respectively. Average annual results are calculated by appropriately scaling the three or

six cycle results assuming seven fuel cycles per year. The calculated maximum annual production yields for the no. 4 and no. 5 designs are 1.138 and 1.393 (22% increase) kg PuO_2, respectively, at qualities (^{238}Pu-to-Pu ratios) of 87.6% and 89.4%. For the constrained case, the annual production yields for the no. 4 and no. 5 designs are 0.678 and 1.105 (63% increase) kg PuO_2, respectively, at qualities of 86.9% and 89.1%. For reasons previously discussed, the target efficiency reduces with increases in the total number of targets loaded.

TABLE II. HFIR reflector design and configuration dependent annual PuO_2 production estimates.

Facility	Quality	PuO_2 (g/target)	Targets per yr.	Annual PuO_2 (g)
permanent reflector no. 4 maximum configuration				
ISVXFs	0.877	4.888	163	798
OSVXFs	0.869	5.480	33	179
LVXFs	0.902	4.910	33	160
Sum	0.876	4.976	229	1138
permanent reflector no. 4 constrained configuration				
ISVXFs	0.870	5.105	98	500
OSVXFs	0.861	5.737	16	94
LVXFs	0.878	5.146	16	84
Sum	0.869	5.189	131	678
permanent reflector no. 5 maximum configuration				
ISVXFs	0.890	4.381	229	1002
OSVXFs	0.882	4.152	25	102
LVXFs	0.907	3.941	74	290
Sum	0.894	4.265	327	1393
permanent reflector no. 5 constrained configuration				
ISVXFs	0.887	4.475	180	804
OSVXFs	0.874	4.927	8	40
LVXFs	0.905	3.992	65	261
Sum	0.891	4.365	253	1105

IV. CONCLUSIONS

^{238}Pu production targets are irradiated in HFIR's PBR, which is replaced every ~ 20 years due to irradiation damage. PBR no. 4 is scheduled to be replaced with PBR no. 5 in 2023; thus, an infrequent opportunity is present to update and improve on the current reflector design. Neutronic and thermal-structural simulations were performed in support of redesigning the reflector to, among other reasons, increase the potential PuO_2 production capability, arrange the VXFs in a layout so as to maintain or increase neutron fluxes down the HB tubes, and enhance the reflector's thermal-structural performance.

The new design increases the number of experiment facilities by six and arranges the facilities in a way to maximize their availability without interfering with other scientific missions. Depending on the assumptions made, it was shown that the annual potential PuO_2 production could increase by ~ 20 – 60% with the new reflector design.

Future work includes performing higher fidelity neutronic production calculations to remove some of the assumptions made in these studies, evaluating alternate target designs for increased production, and qualifying target irradiations in the new reflector.

ACKNOWLEDGMENTS

The authors would like to acknowledge the support for this work provided by NASA's Science Mission Directorate, the US DOE's Office of Nuclear Infrastructure Programs, and ORNL's Research Reactors Division. The authors would also like to thank Charles Daily, ORNL, for his technical review of this paper.

REFERENCES

1. D. Chandler and R. J. Ellis, "Neutronics Simulations of ^{237}Np Targets to Support Safety-Basis and ^{238}Pu Production Assessment Efforts at the High Flux Isotope Reactor," *Proc. NETS 2015*, Albuquerque, NM (2015).
2. X-5 Monte Carlo Team, "MCNP – A general Monte Carlo N-Particle Transport Code, Version 5. Volume I: Overview and Theory," LA-UR-03-1987, Los Alamos National Laboratory (2003).
3. S. W. Mosher, et al., "ADVANTG – An Automated Variance Reduction Parameter Generator," ORNL/TM-2013/416 Rev. 1, Oak Ridge National Laboratory (2015).
4. "SCALE: A Comprehensive Modeling and Simulation Suite for Nuclear Safety Analysis and Design," ORNL/TM-2005/39, Version 6.1, Oak Ridge National Laboratory (2011).
5. W. Haeck, "VESTA User's Manual - Version 2.0.0," IRSN Report DSU/SEC/T/2008-331 Indice A, IRSN, France (2009).
6. "ORIGEN 2.2 – Isotope Generation and Depletion Code Matrix Exponential Method," Oak Ridge National Laboratory (2002).
7. D. Chandler and R. J. Ellis, "Development of an Efficient Approach to Perform Neutronics Simulations for Plutonium-238 Production," *Proc. PHYSOR 2016*, Sun Valley, ID (2016).
8. D. Chandler, B. Betzler, G. Hirtz, G. Ilas, and E. Sunny, "Modeling and Depletion Simulations for a High Flux Isotope Reactor Cycle with a Representative Experiment Loading," ORNL/TM-2016/23, Oak Ridge National Laboratory (2016).
9. B. R. Betzler, et al., "Optimization of Depletion Modeling and Simulation for the High Flux Isotope Reactor," *Proc. M&C 2015*, Nashville, TN (2015).
10. COMSOL Multiphysics® v5.3, www.comsol.com, COMSOL AB, Stockholm, Sweden.